

000 001 002 003 004 005 006 007 008 009 010 011 012 013 014 015 016 017 018 019 020 021 022 023 024 025 026 027 028 029 030 031 032 033 034 035 036 037 038 039 040 041 042 043 044 045 046 047 048 049 050 051 052 053 PICABENCH: HOW FAR ARE WE FROM PHYSICALLY REALISTIC IMAGE EDITING?

Anonymous authors

Paper under double-blind review

ABSTRACT

Image editing has achieved remarkable progress recently. Modern editing models could already follow complex instructions to manipulate the original content. However, beyond completing the editing instructions, the accompanying physical effects are the key to the generation realism. For example, removing an object should also remove its shadow, reflections, and interactions with nearby objects. Unfortunately, existing models and benchmarks mainly focus on instruction completion but overlook these physical effects. So, at this moment, *how far are we from physically realistic image editing?* To answer this, we introduce **PICABench**, which systematically evaluates physical realism across eight sub-dimension (spanning optics, mechanics, and state transitions) for most of the common editing operations (add, remove, attribute change, *etc*). We further propose the **PICAEval**, a reliable evaluation protocol that uses VLM-as-a-judge with per-case, region-level human annotations and questions. Beyond benchmarking, we also explore effective solutions by learning physics from videos and construct a training dataset **PICA-100K**. After evaluating most of the mainstream models, we observe that physical realism remains a challenging problem with large rooms to explore. We hope that our benchmark and proposed solutions can serve as a foundation for future work moving from naive content editing toward physically consistent realism.

1 INTRODUCTION

Recent advances in instruction-based image editing have brought remarkable progress (Wu et al., 2025a; Batifol et al., 2025; OpenAI, 2025; Google, 2025; ByteDance, 2025; Liu et al., 2025; Cai et al., 2025). In particular, with the emergence of unified multi-modal models (Deng et al., 2025; Lin et al., 2025; Wu et al., 2025b), they can seamlessly follow natural language instructions and produce visually compelling, semantically coherent edits. These systems have demonstrated strong generalization capabilities across diverse domains, establishing a new standard for controllable and high-quality image manipulation.

However, the realism of image editing depends not only on semantic accuracy but also on the correct rendering of physical effects. Even simple operations like object addition or removal often trigger complex interactions with lighting, shadows, and object support in the scene. Existing benchmarks overlook this limitation by solely emphasizing semantic fidelity and visual consistency. Although some recent benchmarks (Wu et al., 2025c; Li et al., 2025) attempt to probe scientific-plausible editing capabilities, their test cases diverge from common user-edit scenarios but focus on scientific domains with specific physical or chemistry knowledge. Consequently, we lack a clear understanding of *how far we are from physically realistic image editing*.

To address this gap, we introduce **PICA** (**PhysICs-Aware**) Bench—a diagnostic benchmark designed to evaluate physical realism in image editing beyond semantic fidelity. Drawing on common requirements in real-world editing applications Taesiri et al. (2025), we categorize physical consistency into three intuitive dimensions that are often overlooked in typical editing tasks: *Optics*, *Mechanics*, and *State Transition*. These dimensions were selected to reflect common but under-penalized error types, such as unrealistic lighting effects, impossible object deformations, or implausible state changes. Together, they span eight sub-dimensions, each defined by concrete, checkable criteria: *Optics* includes light propagation, reflection, refraction, and light-source effects; *Mechanics* captures deformation and causality; and *State Transition* addresses both global and local state changes. This

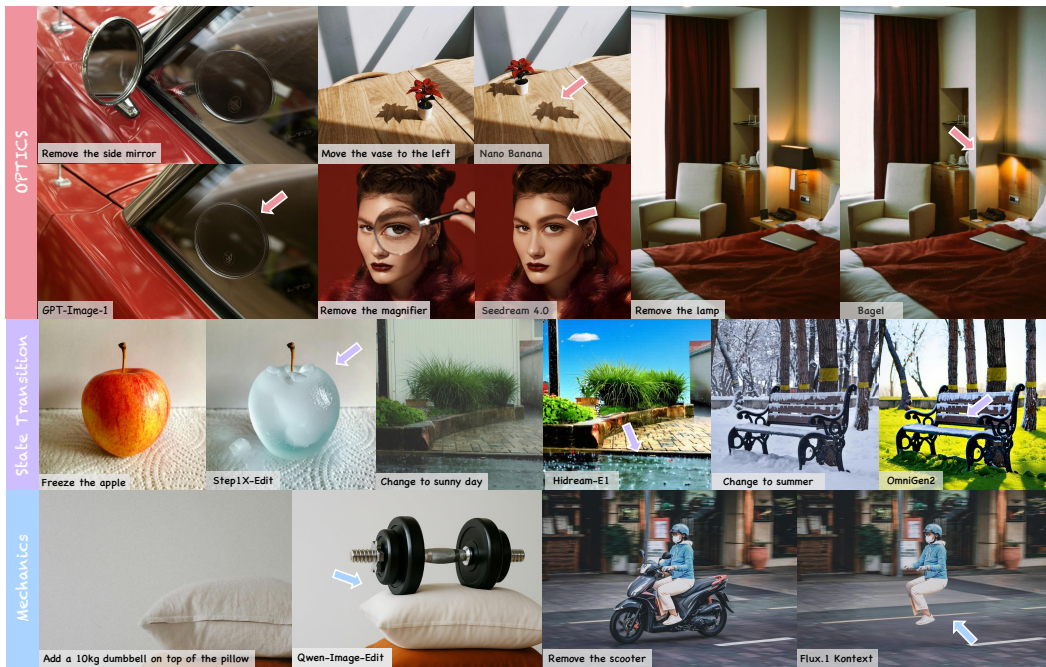


Figure 1: **Challenging cases from PICABench.** Despite providing instruction-aligned outputs, current SoTA models still struggle with generating physically realistic edits, resulting in unharmonized lighting, deformation, or state transitions with *common editing operations*.

fine-grained taxonomy facilitates systematic assessment of whether edited images adhere to principles such as lighting consistency, structural plausibility, and realistic state transitions. Together, it enables comprehensive evaluation and targeted diagnosis of physics violations in image editing models.

With the carefully curated test cases, evaluating the physical correctness remains challenging. We introduce **PICAEval**, a reliable and interpretable protocol tailored for physics-aware assessment. While existing VLM-as-Judge setups (Wu et al., 2025c; Niu et al., 2025; Sun et al., 2025; Zhao et al., 2025) offer a convenient way to automate evaluation, they typically rely on general prompts without grounding in physical principles. As a result, these setups often lack sensitivity to nuanced physical violations and may produce hallucinated judgments when faced with subtle or localized cues. Facing this challenge, PICAEval adopts targeted, per-example **Q&A** aligned with specific physical sub-dimensions, substantially improving diagnostic accuracy. To further reduce hallucination, we incorporate **grounded human-annotated key regions** (e.g., reflection surfaces, contact interfaces), directing the model’s attention to physically relevant evidence. This protocol yields high agreement with human assessments, offering a reliable measurement for physical correctness.

Beyond evaluation, we provide a strong baseline by learning physics from videos. Specifically, we present **PICA-100K**, a synthetic dataset of 100k editing examples constructed from videos. Prior work (Yu et al., 2025b; Chen et al., 2025; Chang et al., 2025; Cao et al., 2025a) has shown that editing pairs derived from videos can enhance the quality and robustness of editing models. Motivated by recent advances in video generation approaching world-simulator (Wan et al., 2025), we design an automatic pipeline that integrates a text-to-image model as a scene renderer and an image-to-video model as a state-transition simulator. From the generated videos, we extract temporally coherent editing pairs and further recalibrate multi-level editing instructions using GPT-5. Our experiments shows that finetuning on PICA-100K significantly improves the baseline model’s capability to generate physically realistic editing results without sacrificing semantic quality.

We benchmark 11 open- and closed-source image editing models across diverse architectures and scales. PICABench comprehensively distinguishes models based on their level of physical awareness, while PICA-100K effectively improves model performance. As shown in Fig. 1, modeling physical realistic transformations is still challenging for current SoTA models, which underlines the significance of advancing from semantic editing toward physically grounded image manipulation in the future. Our main contributions could be summarized as follows.

- 108 • We introduce **PICABench**, a comprehensive and fine-grained benchmark for physics-aware
109 image editing. It covers diversified physical effects (eight sub-dimensions) and includes the
110 great majority of commonly required editing operations in practical applications.
- 111 • We propose **PICAEval**, a region-aware, VQA-based evaluation protocol that incorporates
112 human-annotated key regions to provide interpretable and reliable assessments for physical
113 correctness, improving robustness to subtle errors compared to general scoring prompts.
- 114 • We construct **PICA-100K**, a large-scale dataset derived from synthetic videos, and show
115 that fine-tuning existing models (*e.g.* FLUX.1 Kontext) on this dataset effectively enhances
116 their physical consistency while preserving semantic fidelity.

118 2 RELATED WORK

120 2.1 INSTRUCTION-BASED IMAGE EDITING MODELS

122 Recent advances in instruction-based image editing have led to substantial progress in controllable and
123 diverse visual manipulation (Ye et al., 2025a; Yu et al., 2025a; Zeng et al., 2025; Jin et al., 2024; Huang
124 et al., 2024). Prior approaches implement image editing in a training-free manner (Yang et al., 2023;
125 Pan et al., 2023; Couairon et al., 2022). Recent training-based methods such as HiDream-E1.1 (Cai
126 et al., 2025), StepIX-Edit (Liu et al., 2025), FLUX.1 Kontext (Batifol et al., 2025), and Qwen-Image-
127 Edit (Wu et al., 2025a) improve edit quality, responsiveness, and instruction alignment, while unified
128 frameworks (*e.g.*, Bagel (Deng et al., 2025), OmniGen2 (Wu et al., 2025b), UniWorld-V1 (Lin et al.,
129 2025)) integrate instruction-following, visual reasoning, and multi-task learning to support diverse
130 tasks like free-form manipulation, future-frame prediction, multiview synthesis, segmentation, and
131 composition. Closed-source systems (*e.g.*, GPT-Image-1 OpenAI (2025), Seedream 4.0 (ByteDance,
132 2025), Nano-Banana Google) further demonstrate strong user-intent alignment and high visual fidelity
133 across text-to-image and image-to-image workflows. However, despite these gains, most approaches
134 prioritize semantic and perceptual quality and often neglect physical constraints, leading to artifacts
135 such as unrealistic shadows, refractions, and deformations, underscoring the need for physics-aware
136 editing.

137 2.2 INSTRUCTION-BASED IMAGE EDITING BENCHMARKS

139 Instruction-based image editing benchmarks have evolved from early reliance on semantic (DINO,
140 CLIP (Zhang et al., 2023; Wang et al., 2023; Ma et al., 2024)) and pixel-level (PSNR, SSIM) metrics,
141 which capture similarity but miss fine-grained semantic alignment, to modern “VLM-as-a-Judge”
142 evaluations (Wu et al., 2025c; Niu et al., 2025; Zhao et al., 2025; Sun et al., 2025; Ye et al., 2025b;
143 Liu et al., 2025; Cao et al., 2025b) that use vision-language models to rate instruction adherence,
144 perceptual quality, and realism across diverse, complex prompts. While these LLM-based approaches
145 enable general multi-dimensional scoring, they are prone to overlooking physically implausible
146 edits (*e.g.*, unrealistic lighting, deformations, or object interactions) and can hallucinate, allowing
147 visually appealing yet inconsistent outputs to score well. To close this gap, we introduce a physics-
148 aware benchmark and the PICAEval—a region-grounded, QA-based metric that evaluates physical
149 consistency through localized, interpretable assessments anchored to specific regions of interest.

150 3 METHOD

152 In this section, we first give an overall introduction of PICABench, a benchmark structured to
153 evaluate physical realism in image editing. We then dive into the construction steps, begin with
154 the data curation pipeline, which pairs diverse images with multi-level editing instructions. Next,
155 we present PICAEval, a region-grounded evaluation protocol for reliable assessment. Finally, we
156 propose PICA-100K, a synthetic dataset built from videos, and show how fine-tuning on it provides a
157 strong baseline for improving physics-aware editing.

159 3.1 PICABENCH

160 We introduce the task coverage and overall statistics of PICABench. Our benchmark focuses on three
161 core dimensions of physical realism: *Optics*, *Mechanics*, and *State Transition*, which reflect common

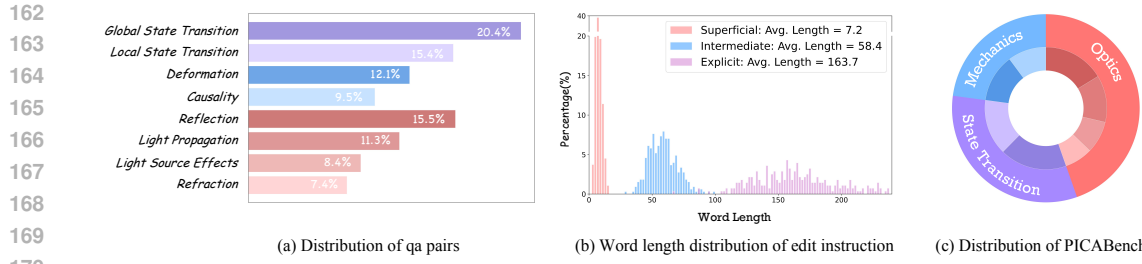


Figure 2: **Statistics Analysis of PICABench.** PICABench is a comprehensive benchmark designed to evaluate physical realism of image editing models across eight sub-dimensions. Fig. 2(a) shows distribution of QA pairs. Fig. 2(b) presents words length distribution of editing instruction across three levels of prompt. Fig. 2(c) provides a perspective on overall composition of PICABench.

yet overlooked failure modes such as unrealistic lighting, implausible deformations, and invalid state changes. As shown in Fig. 2(c), the benchmark includes 984 editing samples spanning these three dimensions, further divided into eight sub-dimensions with concrete and checkable criteria—ranging from optical effects, to mechanical plausibility, and to realistic state transitions.

Optics. This category evaluates whether edited images follow the basic physical rules of light, including how it casts shadows, reflects from surfaces, bends through transparent materials, and interacts with light sources. Edits should produce shadows, reflections, refractions, and light-source effects that align with the scene’s geometry and lighting—matching shadow direction and occlusion, enabling view- and shape-dependent reflections, ensuring smooth background distortion through transparent media, and maintaining consistent color, softness, and falloff for added light sources. These effects, while often subtle, are key to making edits appear natural and physically believable.

Mechanics. This category evaluates whether edited objects remain mechanically and causally consistent with the scene. Deformation should follow material properties—rigid objects must retain shape, while elastic ones deform smoothly with consistent texture and geometry. Causality covers a broader range of physically plausible effects, including structural responses to force redistribution, agent reactions to added or removed stimuli, and environmental changes that alter object behavior, all of which must follow consistent physical or behavioral laws.

State transition. This category evaluates whether environmental and material changes unfold in a physically coherent manner, either across the entire scene or within localized regions. **Global state transitions**, such as changes in time of day, season, or weather, must update all relevant visual cues consistently—ranging from lighting and shadows to vegetation, surface conditions, and atmospheric effects. These changes require coordinated, scene-wide modifications that follow natural temporal or environmental progression. **Local state transitions**, on the other hand, involve targeted physical changes confined to specific objects or regions. These include phenomena such as wetting, drying, melting, burning, freezing, wrinkling, splashing, or fracturing. Edits must integrate smoothly with surrounding context, preserve material boundaries, and maintain plausible causal triggers.

3.2 DATA CURATION

To enable reliable, fine-grained evaluation of physics-aware image editing (PAIE), we curate benchmark entries that pair natural images with editing instructions explicitly designed to test physical consistency. Our data curation pipeline is aligned with the taxonomy in Sec. 3.1 and structured into two stages: *Data Collection* and *Edit Instruction Construction*. A visual overview is shown in Fig. 4.

Data collection. We begin by defining a structured vocabulary mapped to the eight sub-dimensions. To broaden the coverage, we use GPT-5 to expand this vocabulary into a rich keyword set encompassing materials, lighting contexts, and long-tail phenomena. We then use these keywords to retrieve candidate images from licensed and public sources. We prioritize visually diverse scenes that exhibit salient physical cues, such as directional lighting, transparent or reflective media, deformable objects, or phase-changeable substances. Human annotators filter duplicates and artifacts and tag applicable sub-dimensions for each image to support subsequent annotation.



Figure 3: **Statistics Analysis of PICABench.** We present illustrative examples from eight sub-dimensions. Key regions are annotated to help reduce hallucination for VLMs.

Instruction construction. Each retained image is paired with a human-written natural language instruction that induces a physics-relevant edit, grounded in the scene’s physical affordances and designed to implicitly target a specific sub-dimension. To assess not only whether models can follow surface-level commands but also whether they can internalize and apply physical knowledge under varying prompt conditions, we construct three levels of instruction complexity: *superficial* prompts that issue plain edit commands without explanations, *which probe models’ intrinsic physical priors and align with realistic usage scenarios*; *intermediate* prompts that include a brief rationale grounded in physical rules, *serving as reasoning cues to activate physical knowledge*; and *explicit* prompts that further describe the expected results of the edit, *minimizing ambiguity to strictly assess visual capabilities*. We use GPT-5 to expand each human-authored instruction into these three forms, followed by manual review to ensure clarity, factual correctness, and alignment with the visual context. For each sample, the benchmark retains a canonical version of the instruction.

3.3 PICAEVAL

Evaluating physics-aware image editing (PAIE) remains challenging. Unlike semantic fidelity or perceptual quality, physical realism is inherently contextual: it depends not only on the edited content but also on its alignment with the physical constraints implied by the original scene and instruction. Moreover, there is no reference image to serve as ground truth, and general prompting strategies such as “Is this edit correct?” often yield vague or hallucinated responses from VLMs.

To address this, we introduce **PICAEval**, a region-grounded, question-answering based metric designed to assess physical consistency in a modular, interpretable manner. Inspired by recent metrics like VDCscore (Chai et al., 2024), PICAEval decomposes each evaluation instance into multiple region-specific verification questions that can be reliably judged by a VLM. Each benchmark entry is paired with a curated set of spatially grounded yes/no questions designed to probe whether the edited output image preserves physical plausibility within key regions. These questions are tied to visually observable physical phenomena—such as shadows, reflections, object contact, or material deformation—and are anchored to human-annotated regions of interest (ROIs). This design

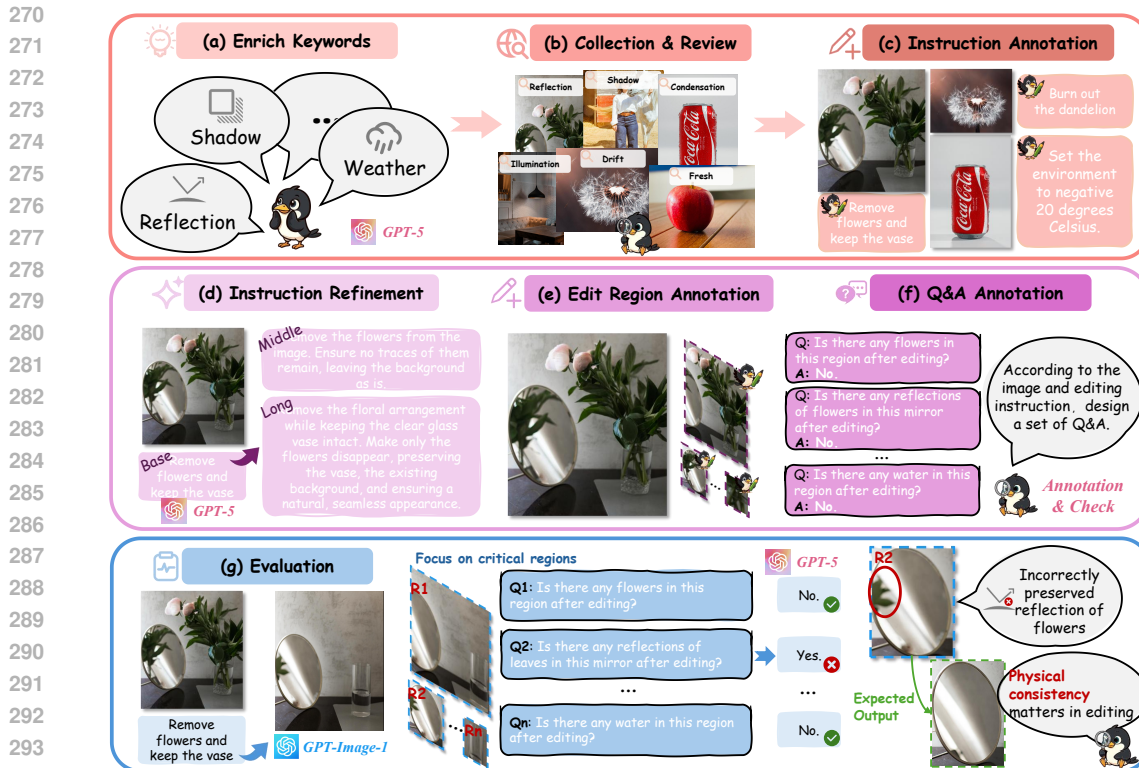


Figure 4: **Overall pipeline for benchmarks construction and evaluation.** (a–b) We enrich a physics-specific keyword set and retrieve diverse candidate images. (c–d) Human-written editing instructions are expanded into three levels of complexity using GPT-5. (e) Annotators mark physics-critical regions. (f) Spatially grounded yes/no questions are generated to evaluate physical plausibility. (g) During evaluation, VLMs answer each question with reference to the edited region.

encourages localized, evidence-based reasoning and reduces the influence of irrelevant image content on the VLM’s judgment.

Evaluation pipeline. As illustrated in Fig. 4(e–f), the evaluation proceeds as follows: (1) Annotators mark key regions in the input image where physics-critical evidence is expected to appear post-editing (e.g., reflective surfaces, deformation zones, cast shadows); (2) Using the edit instruction and region, GPT-5 generates a set of 4–5 binary QA pairs per entry, which are then manually reviewed for clarity and coverage; (3) At test time, a VLM (e.g., GPT-5) is prompted with the edited image, instruction, region, and question, and produces an answer constrained to the visible content within the region.

PICAEval is computed as the proportion of questions for which the VLM answer exactly matches the reference label. Compared to direct prompting, this QA-based protocol offers three key advantages: (i) spatial grounding reduces hallucination, (ii) decomposition increases interpretability and robustness, and (iii) the format better mirrors how humans evaluate physical plausibility—through concrete, localized checks. We report quantitative comparisons and per-subdimension breakdowns to enable diagnostic analysis of physics-aware image editing capabilities in Sec. 4.

3.4 STRONG BASELINE: LEARNING PHYSICAL REALISM FROM VIDEOS

To address the limitations identified in Sec. 3.1, we introduce **PICA-100K**, a purely synthetic dataset designed to improve physics-aware image editing. Our decision to use fully generated data is driven by three primary motivations. **First**, prior work (Yu et al., 2025b; Chen et al., 2025; Cao et al., 2025a; Chang et al., 2025) has demonstrated that constructing image-editing data from video is an effective strategy for enhancing model performance, particularly for capturing real world dynamics. **Second**, building large-scale, real-world datasets tailored to physics-aware editing is prohibitively expensive and labor-intensive. **Third**, the rapid progress in generative modeling has unlocked new



Figure 5: **PICA-100K construction pipeline.** We first curate structured prompts for scene and subject composition, refined by GPT-5 and rendered using FLUX.1-Krea-dev for text-to-image generation. Motion-based edit instructions are created via GPT-5 and applied using Wan2.2-14B to synthesize short videos depicting physical transformations. The first and last frames, along with the edit instruction, form the image pairs for training.

possibilities: state-of-the-art text-to-image models (Labs, 2024) can now generate highly realistic and diverse images, while powerful image-to-video (I2V) models such as Wan2.2-14B (Wan et al., 2025) simulate complex dynamic processes with remarkable physical fidelity. Together, these generative priors enable the creation of training data with precise and controllable supervision signals, which are essential for training models to perform fine-grained, physically realistic edits. We find that fine-tuning the baseline on PICA-100K enhances the model’s performance in real-world evaluation.

PICA-100K dataset. As shown in Fig. 5, we begin by constructing two structured prompt dictionaries: a Subject Dictionary and a Scene Dictionary, which include a wide array of subjects and environments (e.g., “a tea pot,” “a black kitchen table”). These entries are paired using handcrafted text-to-image (T2I) templates and further refined using GPT-5, resulting in high-quality natural language instructions. The refined instructions are passed to the FLUX.1-Krea-dev (Lee et al., 2025) to generate static source images that are both visually realistic and semantically diverse.

Next, we generate motion-oriented instructions to simulate physical edits. This is accomplished by designing a series of I2V instruction templates, describing plausible motion-based changes such as rotations, movements, or tilts. These templates are expanded using GPT-5 to improve clarity and behavioral precision. The motion instructions (e.g., “remove the tea pot,” “tilt the vase until it tips over,” or “swing the lantern gently in the wind”) are then applied to the corresponding images using Wan2.2-14B-I2V, which synthesizes short video clips depicting the intended physical transformations.

For each video, we extract the first and last frames to construct a (source, edited) image pair. These pairs, along with the corresponding instruction, are used to form supervision signals. GPT-5 is employed to annotate each pair automatically, labeling the final frame as the preferred output. This pipeline eliminates the need for manual labeling while maintaining high annotation consistency.

Our final dataset contains 100,000 instruction-based editing samples distributed across eight physics categories. The experimental results in Sec. 4 demonstrate that this pipeline can effectively generate high-quality data, significantly enhancing model performance on physics-aware image editing tasks.

Comparison with related works. PICA-100K is closely related to recent efforts Chang et al. (2025); Rotstein et al. (2025) that utilize video priors on image editing tasks. It differs from them in both motivation and methodology. ByteMorph (Chang et al., 2025) is primarily designed for non-rigid image editing, emphasizing visually salient motions such as articulation, deformation, and large pose or viewpoint changes. However, focus on large motions may hurt models’ ability to keep non-edited region unchanged. Rotstein et al. (2025) proposes a training-free method, which focuses on zero-shot feasibility. It directly leverages a video generation model to simulate the editing process. Our work instead targets physical realism, which represents implicit physics principle of real world. Also, our data pipeline allows for more controllable generation where the non-edited regions remain stable.

Training paradigm. To demonstrate the effectiveness of PICA-100K, we fine-tune FLUX.1-Kontext-dev (Batifol et al., 2025), a 12B flow-based diffusion transformer for image editing. We employ LoRA (Hu et al., 2022) with a rank of 256 for fine-tuning. The model is trained using a batch size of 64 and optimized using the AdamW optimizer with a learning rate of 10^{-5} . The entire fine-tuning procedure is conducted over 10,000 optimization steps on 8 NVIDIA H200 GPUs.

378 Table 1: **Quantitative comparison on PICABench evaluated by GPT-5** for instruction-based editing
 379 models, where Acc \uparrow , Con \uparrow , LP, LSE, GST, LST denote Accuracy (%) and Consistency (db), Light
 380 propagation, Light Source Effects, Global State Transition, Local State Transition respectively. █
 381 and █ indicates the best and second best score in a category, respectively.

Model	LP		LSE		Reflection		Refraction		Deformation		Causality		GST		LST		Overall	
	Acc \uparrow	Con \uparrow	Acc \uparrow	Con \uparrow	Acc \uparrow	Con \uparrow	Acc \uparrow	Con \uparrow	Acc \uparrow	Con \uparrow	Acc \uparrow	Con \uparrow	Acc \uparrow	Con \uparrow	Acc \uparrow	Con \uparrow	Acc \uparrow	Con \uparrow
GPT-Image-1	55.65	18.81	66.75	20.13	64.05	19.07	43.36	18.64	62.42	20.37	50.00	20.08	73.87	36.32	58.72	22.71	61.46	22.95
Nano Banana	50.00	29.72	54.63	31.39	63.79	26.90	35.50	27.74	57.45	27.42	52.11	28.44	64.38	40.63	56.25	32.81	56.46	31.22
Seedream 4.0	54.77	25.49	65.80	28.27	68.69	23.82	38.75	27.00	59.11	27.27	51.05	26.71	71.14	36.76	58.98	33.20	60.84	29.05
Bagel	43.82	28.57	51.54	32.08	56.96	28.78	29.00	24.31	44.87	28.08	40.51	31.20	55.09	35.15	43.75	32.05	47.52	30.48
Bagel-Think	43.46	31.33	55.34	29.80	55.67	33.01	35.77	27.66	48.51	29.79	42.62	34.11	53.62	36.91	48.05	34.19	49.10	32.70
DiMOO	36.75	27.70	33.97	33.26	30.28	24.00	26.56	23.93	33.77	30.65	32.49	27.39	21.23	49.42	24.35	36.09	28.92	32.73
OmniGen2	46.29	20.46	49.41	28.85	58.76	25.10	27.37	23.22	44.21	25.51	40.93	28.05	49.71	38.52	34.90	27.80	45.28	27.84
Uniworld-V1	37.99	18.89	42.99	20.48	48.71	19.16	26.29	19.06	42.05	19.16	33.76	18.10	31.80	17.54	33.20	19.56	37.30	18.90
Hidream-E1	43.46	20.46	52.26	25.38	59.15	20.18	32.52	21.17	47.19	22.37	39.45	22.15	61.06	34.75	45.18	24.17	49.76	24.39
Step1X-Edit	42.05	29.46	53.68	31.26	58.89	29.50	30.89	31.58	48.34	31.51	49.79	32.09	58.02	35.43	47.53	30.19	50.42	31.47
Qwen-Image-Edit	52.12	22.03	59.14	26.28	64.82	23.80	35.50	26.54	50.50	26.42	48.95	24.94	63.60	36.72	54.17	28.44	55.62	27.42
Flux.1 Kontext	48.23	29.21	57.48	29.61	62.24	27.83	28.46	28.22	51.32	31.50	51.05	31.44	53.82	39.03	45.31	33.95	51.06	31.90
Flux.1 Kontext+SFT	49.12	30.42	59.38	30.69	64.95	28.37	30.89	28.40	50.17	31.74	46.62	31.87	51.17	40.82	44.79	34.41	51.88	32.71

394 Table 2: **Performance across different prompt specificity levels.** Model performance improves
 395 with prompt specificity.

Model	LP		LSE		Reflection		Refraction		Deformation		Causality		GST		LST		Overall	
	Acc \uparrow	Con \uparrow	Acc \uparrow	Con \uparrow	Acc \uparrow	Con \uparrow	Acc \uparrow	Con \uparrow	Acc \uparrow	Con \uparrow	Acc \uparrow	Con \uparrow	Acc \uparrow	Con \uparrow	Acc \uparrow	Con \uparrow	Acc \uparrow	Con \uparrow
Bagel-superficial	46.42	36.17	42.43	39.84	48.11	35.18	46.85	30.10	44.56	36.43	44.76	37.64	43.54	35.66	41.85	36.47	44.62	36.28
Bagel-intermediate	53.96	26.28	62.15	22.93	54.95	30.73	48.95	22.92	54.01	26.49	42.89	30.14	53.79	34.00	40.84	28.55	51.21	28.97
Bagel-explicit	58.03	17.63	66.90	18.44	57.90	20.95	51.40	18.68	58.29	18.81	53.37	23.71	66.12	33.53	57.00	21.41	59.56	23.06
Flux.1 Kontext-superficial	51.06	29.70	59.33	29.96	52.71	28.85	41.61	28.49	51.52	32.11	40.19	33.89	47.18	37.84	38.53	31.92	47.47	32.39
Flux.1 Kontext-intermediate	50.68	28.15	62.68	27.77	54.83	28.46	34.97	28.71	52.23	30.09	49.33	31.07	48.07	38.13	43.87	31.69	50.19	31.28
Flux.1 Kontext-explicit	57.64	27.77	66.90	25.25	59.67	27.35	40.21	26.96	56.51	28.67	57.74	27.99	65.68	36.11	52.24	29.57	59.11	29.40
Qwen-Image-Edit-superficial	58.99	22.61	64.08	27.43	62.62	23.86	60.84	25.06	54.37	24.65	48.18	26.79	62.85	35.42	52.53	25.75	57.99	27.24
Qwen-Image-Edit-intermediate	60.93	23.62	67.78	24.82	60.58	24.82	46.50	27.22	57.58	27.49	51.30	26.66	60.55	36.20	50.51	28.24	57.56	28.06
Qwen-Image-Edit-explicit	57.06	20.18	69.72	22.79	63.08	22.63	52.10	26.10	58.11	24.95	59.29	23.99	66.79	35.03	60.46	25.08	62.09	25.78
Nano Banana-superficial	55.71	29.32	58.80	32.21	56.37	27.67	48.25	27.31	59.54	28.31	54.17	30.17	59.51	39.00	52.24	30.18	56.32	31.29
Nano Banana-intermediate	56.48	28.89	62.85	30.70	58.96	28.06	46.85	28.12	61.68	27.96	60.12	28.12	61.59	38.56	53.68	30.54	58.96	30.74
Nano Banana-explicit	59.00	29.01	62.15	30.04	61.67	27.43	51.40	27.97	62.57	28.52	63.45	29.14	61.14	38.66	56.57	31.02	60.62	30.90

4 EXPERIMENT

4.1 EVALUATION DETAILS

We evaluate 11 closed- and open-source models, covering most recent image-editing and unified vision-language systems. Closed-source systems include GPT-Image-1 (OpenAI, 2025), Nano Banana (Google, 2025), and Seedream 4.0 (ByteDance, 2025). Open-source baselines include FLUX.1 Kontext (Batifol et al., 2025), Step1X-Edit (Liu et al., 2025), Bagel (Deng et al., 2025), Bagel-Think (Deng et al., 2025), HiDream-E1.1 (Cai et al., 2025), UniWorld-V1 (Lin et al., 2025), OmniGen2 (Wu et al., 2025b), Qwen-Image-Edit (Wu et al., 2025a), and DiMOO (Team, 2025). All input images are resized proportionally to a maximum resolution of 1024 on the longer side prior to evaluation. To ensure fairness and reproducibility, we run all models using their default settings from official repositories or web APIs on H200 GPUs.

For PICAEval, we first use the provided annotation masks to crop the edited region from the image. The cropped region is then resized proportionally to 1024 on the longer side before being passed to the VQA-based evaluator. This ensures standardized input size while preserving relevant physical cues within the editing region. We report results using both the current state-of-the-art closed-source model (GPT-5) and the leading open-source alternative (Qwen2.5-VL-72B) as VLM evaluator. For consistency evaluation, we compute PSNR over the non-edited regions by masking out the predicted edit area, thereby measuring how well models preserve the original content outside the editing scope.

4.2 BENCHMARK RESULTS

We are still far from physically realistic image editing. Tab. 1 presents a comprehensive evaluation of existing methods. All open-source models score below 60 on the benchmark, and only the closed-source models—GPT-Image-1 and Seedream 4.0—slightly exceed this threshold. These results

432 **Table 3: Ablation Results.** We construct a real-video-based dataset (Mira400K). The model trained
 433 on Mira400K underperforms, highlighting the effectiveness of our targeted synthetic data pipeline.

Model	LP		LSE		Reflection		Refraction		Deformation		Causality		GST		LST		Overall	
	Acc ↑	Con ↑	Acc ↑	Con ↑	Acc ↑	Con ↑	Acc ↑	Con ↑	Acc ↑	Con ↑	Acc ↑	Con ↑	Acc ↑	Con ↑	Acc ↑	Con ↑	Acc ↑	Con ↑
Flux.1 Kontext	66.06	29.46	70.28	30.76	71.40	28.31	43.46	29.59	58.66	31.48	57.29	32.30	63.41	36.39	56.16	32.01	61.98	31.66
+MIRA400K	63.11	27.53	70.08	29.75	70.90	26.87	44.65	28.64	60.61	29.77	53.06	30.59	61.97	38.23	54.37	30.69	60.60	30.71
+PICA100K	69.45	29.92	73.98	31.19	74.60	27.99	47.34	28.92	64.87	31.54	57.95	32.34	66.37	37.94	60.15	32.42	65.19	31.99

439 underscore a persistent gap in the ability of current image editing models to generate physics-aware
 440 and physically realistic outputs.

441 **The gap between understanding and physical realism.** Among open-source models, unified
 442 architectures consistently underperform compared to dedicated image editing models. Although
 443 unified MLLMs attempt to integrate visual understanding and generation within a single framework,
 444 the presumed advantage of enhanced world understanding does not translate into improved physical
 445 realism. This suggests that stronger understanding alone is insufficient, and effectively coupling
 446 understanding with generation remains an open challenge. Tab. 2 presents performance across
 447 different prompt specificity levels. As shown in Tab. 2, model **accuracy** improves as prompts become
 448 more detailed. **The decrease of consistency can be attributed to the trade-off between improving**
 449 **physical realism and preserving non-edited image regions.** However, the gain from intermediate
 450 prompts is much smaller than that from explicit prompts. We speculate this is due to the lack of
 451 internalized physics principles, which prevents models from leveraging the additional information.
 452 Interestingly, the Bagel model outperforms Flux Kontext under explicit prompts, likely because its
 453 unified architecture enhances long-text comprehension. Notably, even with explicit prompts that
 454 explicitly specify the editing regions, the overall performance still remains below 60.

455 **Video data helps physics learning.** Fine-tuning FLUX.1-KONTEXT on our PICA-100K dataset
 456 yields consistent improvements across multiple dimensions of physical realism. As shown in Ap-
 457 pendix A.5, our model consistently produces more physically plausible results, while other models
 458 often exhibit unrealistic lighting effects, implausible object deformations, or invalid state changes.
 459 Quantitative results in Tab. 1 further support this: our fine-tuned model achieves a +2.01% im-
 460 provement in optics accuracy and a +0.27% gain in mechanics accuracy over the base model. In addition, it
 461 demonstrates better overall physical consistency, improving from 31.90% to 32.71%. These findings
 462 suggest that synthetic supervision signals derived from videos can effectively enhance a model’s
 463 capacity for physics-aware image editing. They also validate the effectiveness of our video-to-image
 464 data generation pipeline in capturing diverse and complex physical phenomena. However, we observe
 465 a slight drop in State Transition Accuracy, possibly due to limitations in directly using first and
 466 last frames of a video to represent meaningful state changes. We plan to explore more fine-grained
 467 strategies to extract temporal context and leverage intermediate frames.

468 We also experimented with using real video data to construct an image editing dataset. Following
 469 the data pipeline of Unireal (Chen et al., 2025), we employed Miradata (Ju et al., 2024) to generate
 470 400K edited images (Mira400K) and trained the model under the same settings. However, as shown
 471 in Tab. 3, the model trained on Mira400K performed even worse in overall accuracy. This further
 472 demonstrates the efficiency and effectiveness of our proposed data generation pipeline.

4.3 VALIDITY OF PICAEval

474 We conduct a human study using Elo ranking to further validate the effectiveness of PICAEval. As
 475 shown in Fig. 6, PICAEval achieves higher correlation with human judgments than the baseline.
 476 This result demonstrates that our per-case, region-level human annotations and carefully designed
 477 questions effectively mitigate VLM hallucinations, leading to outcomes that better reflect human
 478 preferences. Additional details of the human study are provided in Appendix A.4.

5 LIMITATIONS AND FUTURE DIRECTIONS

484 While our approach demonstrates clear benefits in physics-aware image editing, it has several
 485 limitations. First, the PICA-100K dataset, though effective, is built using a relatively simple generation
 486 pipeline and remains limited in scale. Second, our model is trained purely via supervised finetuning

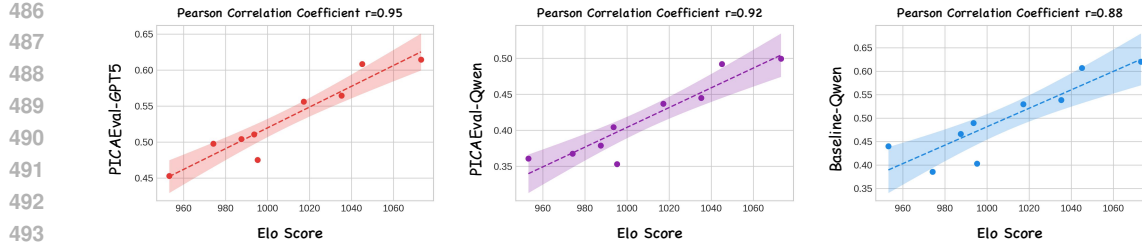


Figure 6: **Alignment between evaluation results and human preference.** We make Pearson correlation analysis between Elo scores from human study and different settings. PICAEval-GPT5, PICAEval-Qwen use GPT-5 and Qwen2.5-VL-72B as the evaluator respectively. Baseline-Qwen adopts Qwen2.5-VL-72B but without edit region annotations. Results show that incorporating stronger VLMs and region-level information yields higher alignment with human preference.

(SFT), which brings modest gains but may underexploit the full potential of data. Third, the current framework only supports single-image inputs, lacking the ability to incorporate multi-image or multi-condition contexts. In future work, we aim to enhance the data pipeline, explore RL-based post-training, and extend the model to support more expressive conditioning formats.

6 CONCLUSION

We present PICABench, a new benchmark for evaluating physical realism in image editing, along with PICAEval, a region-grounded, QA-based metric for fine-grained assessment. Our results show that current models, still far from producing physically realistic edits. To improve this, we introduce PICA-100K, a synthetic dataset derived from videos. Fine-tuning on this dataset significantly boosts physical consistency, demonstrating the promise of video-based supervision. We hope our benchmark, metric, and dataset can drive progress toward physics-aware image editing.

540 REFERENCES
541

542 Shuai Bai, Keqin Chen, Xuejing Liu, Jialin Wang, Wenbin Ge, Sibo Song, Kai Dang, Peng Wang,
543 Shijie Wang, Jun Tang, Humen Zhong, Yuanzhi Zhu, Mingkun Yang, Zhaohai Li, Jianqiang Wan,
544 Pengfei Wang, Wei Ding, Zheren Fu, Yiheng Xu, Jiabo Ye, Xi Zhang, Tianbao Xie, Zesen Cheng,
545 Hang Zhang, Zhibo Yang, Haiyang Xu, and Junyang Lin. Qwen2.5-v1 technical report. *arXiv*
546 *preprint arXiv:2502.13923*, 2025.

547 Stephen Batifol, Andreas Blattmann, Frederic Boesel, Saksham Consul, Cyril Diagne, Tim Dockhorn,
548 Jack English, Zion English, Patrick Esser, Sumith Kulal, et al. Flux. 1 kontext: Flow matching for
549 in-context image generation and editing in latent space. *arXiv e-prints*, 2025.

550 ByteDance. Seedream 4.0. 2025. URL https://seed/bytedance.com/en/seedream4_0/.

553 Qi Cai, Jingwen Chen, Yang Chen, Yehao Li, Fuchen Long, Yingwei Pan, Zhaofan Qiu, Yiheng
554 Zhang, Fengbin Gao, Peihan Xu, et al. Hidream-i1: A high-efficient image generative foundation
555 model with sparse diffusion transformer. *arXiv preprint arXiv:2505.22705*, 2025.

556 Mingdeng Cao, Xuaner Zhang, Yinjiang Zheng, and Zhihao Xia. Instruction-based image manipula-
557 tion by watching how things move. In *Proceedings of the Computer Vision and Pattern Recognition*
558 Conference, pp. 2704–2713, 2025a.

559 Shuo Cao, Nan Ma, Jiayang Li, Xiaohui Li, Lihao Shao, Kaiwen Zhu, Yu Zhou, Yuandong Pu,
560 Jiarui Wu, Jiaquan Wang, Bo Qu, Wenhui Wang, Yu Qiao, Dajun Yao, and Yihao Liu. Artimuse:
561 Fine-grained image aesthetics assessment with joint scoring and expert-level understanding, 2025b.
562 URL <https://arxiv.org/abs/2507.14533>.

563 Wenhao Chai, Enxin Song, Yilun Du, Chenlin Meng, Vashisht Madhavan, Omer Bar-Tal, Jenq-Neng
564 Hwang, Saining Xie, and Christopher D Manning. Auroracap: Efficient, performant video detailed
565 captioning and a new benchmark. *arXiv preprint arXiv:2410.03051*, 2024.

566 Di Chang, Mingdeng Cao, Yichun Shi, Bo Liu, Shengqu Cai, Shijie Zhou, Weilin Huang, Gordon
567 Wetzstein, Mohammad Soleymani, and Peng Wang. Bytemorph: Benchmarking instruction-guided
568 image editing with non-rigid motions. *arXiv preprint arXiv:2506.03107*, 2025.

569 Xi Chen, Zhifei Zhang, He Zhang, Yuqian Zhou, Soo Ye Kim, Qing Liu, Yijun Li, Jianming Zhang,
570 Nanxuan Zhao, Yilin Wang, et al. Unireal: Universal image generation and editing via learning
571 real-world dynamics. In *Proceedings of the Computer Vision and Pattern Recognition Conference*,
572 pp. 12501–12511, 2025.

573 Guillaume Couairon, Jakob Verbeek, Holger Schwenk, and Matthieu Cord. Diffedit: Diffusion-based
574 semantic image editing with mask guidance. *arXiv preprint arXiv:2210.11427*, 2022.

575 Chaorui Deng, Deyao Zhu, Kunchang Li, Chenhui Gou, Feng Li, Zeyu Wang, Shu Zhong, Weihao
576 Yu, Xiaonan Nie, Ziang Song, et al. Emerging properties in unified multimodal pretraining. *arXiv*
577 *preprint arXiv:2505.14683*, 2025.

578 Google. Nano banana. 2025. URL [https://gemini.google/overview/
579 image-generation/](https://gemini.google/overview/image-generation/).

580 Edward J Hu, Yelong Shen, Phillip Wallis, Zeyuan Allen-Zhu, Yuanzhi Li, Shean Wang, Lu Wang,
581 Weizhu Chen, et al. Lora: Low-rank adaptation of large language models. *Proceedings of the*
582 *International Conference on Learning Representations (ICLR)*, 2022.

583 Yuzhou Huang, Liangbin Xie, Xintao Wang, Ziyang Yuan, Xiaodong Cun, Yixiao Ge, Jiantao Zhou,
584 Chao Dong, Rui Huang, Ruimao Zhang, et al. Smartedit: Exploring complex instruction-based
585 image editing with multimodal large language models. In *Proceedings of the IEEE/CVF Conference*
586 *on Computer Vision and Pattern Recognition*, pp. 8362–8371, 2024.

587 Ying Jin, Pengyang Ling, Xiaoyi Dong, Pan Zhang, Jiaqi Wang, and Dahu Lin. Reasonpix2pix:
588 instruction reasoning dataset for advanced image editing. *arXiv preprint arXiv:2405.11190*, 2024.

594 Xuan Ju, Yiming Gao, Zhaoyang Zhang, Ziyang Yuan, Xintao Wang, Ailing Zeng, Yu Xiong, Qiang
 595 Xu, and Ying Shan. Miradata: A large-scale video dataset with long durations and structured
 596 captions. *Advances in Neural Information Processing Systems*, 37:48955–48970, 2024.

597

598 Black Forest Labs. Flux. <https://github.com/black-forest-labs/flux>, 2024.

599

600 Sangwu Lee, Titus Ebbecke, Erwann Millon, Will Beddow, Le Zhuo, Iker García-Ferrero, Liam
 601 Esparraguera, Mihai Petrescu, Gian Saß, Gabriel Menezes, and Victor Perez. Flux.1 krea [dev].
 602 <https://github.com/krea-ai/flux-krea>, 2025.

603

604 Jialuo Li, Wenhao Chai, Xingyu Fu, Haiyang Xu, and Saining Xie. Science-t2i: Addressing scientific
 605 illusions in image synthesis, 2025. URL <https://arxiv.org/abs/2504.13129>.

606

607 Bin Lin, Zongjian Li, Xinhua Cheng, Yuwei Niu, Yang Ye, Xianyi He, Shenghai Yuan, Wangbo Yu,
 608 Shaodong Wang, Yunyang Ge, et al. Uniworld: High-resolution semantic encoders for unified
 609 visual understanding and generation. *arXiv preprint arXiv:2506.03147*, 2025.

610

611 Shiyu Liu, Yucheng Han, Peng Xing, Fukun Yin, Rui Wang, Wei Cheng, Jiaqi Liao, Yingming Wang,
 612 Honghao Fu, Chunrui Han, et al. Step1x-edit: A practical framework for general image editing.
 613 *arXiv preprint arXiv:2504.17761*, 2025.

614

615 Yiwei Ma, Jiayi Ji, Ke Ye, Weihuang Lin, Zhibin Wang, Yonghan Zheng, Qiang Zhou, Xiaoshuai
 616 Sun, and Rongrong Ji. I2ebench: A comprehensive benchmark for instruction-based image editing.
 617 *Advances in Neural Information Processing Systems (NeurIPS)*, 37:41494–41516, 2024.

618

619 Yuwei Niu, Munan Ning, Mengren Zheng, Weiyang Jin, Bin Lin, Peng Jin, Jiaqi Liao, Kunpeng Ning,
 620 Chaoran Feng, Bin Zhu, and Li Yuan. Wise: A world knowledge-informed semantic evaluation for
 621 text-to-image generation. *arXiv preprint arXiv:2503.07265*, 2025.

622

623 OpenAI. Gpt-image-1. 2025. URL <https://openai.com/index/introducing-4o-image-generation/>.

624

625 Zhihong Pan, Riccardo Gherardi, Xiufeng Xie, and Stephen Huang. Effective real image editing with
 626 accelerated iterative diffusion inversion. In *Proceedings of the IEEE International Conference on
 627 Computer Vision (ICCV)*, pp. 15912–15921, 2023.

628

629 Noam Rotstein, Gal Yona, Daniel Silver, Roy Velich, David Bensaid, and Ron Kimmel. Pathways on
 630 the image manifold: Image editing via video generation. In *Proceedings of the Computer Vision
 631 and Pattern Recognition Conference*, pp. 7857–7866, 2025.

632

633 Kaiyue Sun, Rongyao Fang, Chengqi Duan, Xian Liu, and Xihui Liu. T2i-reasonbench: Benchmark-
 634 reasoning reasoning-informed text-to-image generation. *arXiv preprint arXiv:2508.17472*, 2025.

635

636 Mohammad Reza Taesiri, Brandon Collins, Logan Bolton, Viet Dac Lai, Franck Dernoncourt, Trung
 637 Bui, and Anh Totti Nguyen. Understanding generative ai capabilities in everyday image editing
 638 tasks. *arXiv preprint arXiv:2505.16181*, 2025.

639

640 Alpha VLLM Team. Lumina-dimoo: A unified masked diffusion model for multi-modal generation
 641 and understanding, 2025. URL <https://github.com/Alpha-VLLM/Lumina-DiMOO>.

642

643 Team Wan, Ang Wang, Baole Ai, Bin Wen, Chaojie Mao, Chen-Wei Xie, Di Chen, Feiwu Yu,
 644 Haiming Zhao, Jianxiao Yang, et al. Wan: Open and advanced large-scale video generative models.
 645 *arXiv preprint arXiv:2503.20314*, 2025.

646

647 Su Wang, Chitwan Saharia, Ceslee Montgomery, Jordi Pont-Tuset, Shai Noy, Stefano Pellegrini,
 648 Yasumasa Onoe, Sarah Laszlo, David J Fleet, Radu Soricut, et al. Imagen editor and editbench:
 649 Advancing and evaluating text-guided image inpainting. In *Proceedings of the IEEE Conference
 650 on Computer Vision and Pattern Recognition (CVPR)*, pp. 18359–18369, 2023.

651

652 Chenfei Wu, Jiahao Li, Jingren Zhou, Junyang Lin, Kaiyuan Gao, Kun Yan, Sheng-ming Yin, Shuai
 653 Bai, Xiao Xu, Yilei Chen, et al. Qwen-image technical report. *arXiv preprint arXiv:2508.02324*,
 654 2025a.

648 Chenyuan Wu, Pengfei Zheng, Ruiran Yan, Shitao Xiao, Xin Luo, Yueze Wang, Wanli Li, Xiyan
 649 Jiang, Yexin Liu, Junjie Zhou, et al. Omnipgen2: Exploration to advanced multimodal generation.
 650 *arXiv preprint arXiv:2506.18871*, 2025b.

651 Yongliang Wu, Zonghui Li, Xinting Hu, Xinyu Ye, Xianfang Zeng, Gang Yu, Wenbo Zhu, Bernt
 652 Schiele, Ming-Hsuan Yang, and Xu Yang. Kris-bench: Benchmarking next-level intelligent image
 653 editing models. *arXiv preprint arXiv:2505.16707*, 2025c.

654 Binxin Yang, Shuyang Gu, Bo Zhang, Ting Zhang, Xuejin Chen, Xiaoyan Sun, Dong Chen, and Fang
 655 Wen. Paint by example: Exemplar-based image editing with diffusion models. In *Proceedings
 656 of the IEEE Conference on Computer Vision and Pattern Recognition (CVPR)*, pp. 18381–18391,
 657 2023.

658 Junyan Ye, Dongzhi Jiang, Zihao Wang, Leqi Zhu, Zhenghao Hu, Zilong Huang, Jun He, Zhiyuan
 659 Yan, Jinghua Yu, Hongsheng Li, et al. Echo-4o: Harnessing the power of gpt-4o synthetic images
 660 for improved image generation. *arXiv preprint arXiv:2508.09987*, 2025a.

661 Yang Ye, Xianyi He, Zongjian Li, Bin Lin, Shenghai Yuan, Zhiyuan Yan, Bohan Hou, and Li Yuan.
 662 Imgedit: A unified image editing dataset and benchmark. *arXiv preprint arXiv:2505.20275*, 2025b.

663 Qifan Yu, Wei Chow, Zhongqi Yue, Kaihang Pan, Yang Wu, Xiaoyang Wan, Juncheng Li, Siliang
 664 Tang, Hanwang Zhang, and Yuetong Zhuang. Anyedit: Mastering unified high-quality image
 665 editing for any idea. In *Proceedings of the Computer Vision and Pattern Recognition Conference*,
 666 pp. 26125–26135, 2025a.

667 Xin Yu, Tianyu Wang, Soo Ye Kim, Paul Guerrero, Xi Chen, Qing Liu, Zhe Lin, and Xiaojuan Qi.
 668 Objectmover: Generative object movement with video prior. In *Proceedings of the Computer
 669 Vision and Pattern Recognition Conference*, pp. 17682–17691, 2025b.

670 Bohan Zeng, Ling Yang, Jiaming Liu, Minghao Xu, Yuanxing Zhang, Pengfei Wan, Wentao Zhang,
 671 and Shuicheng Yan. Editworld: Simulating world dynamics for instruction-following image editing.
 672 In *Proceedings of the 33rd ACM International Conference on Multimedia*, pp. 12674–12681, 2025.

673 Kai Zhang, Lingbo Mo, Wenhui Chen, Huan Sun, and Yu Su. Magicbrush: A manually annotated
 674 dataset for instruction-guided image editing. In *Advances in Neural Information Processing
 675 Systems*, 2023.

676 Xiangyu Zhao, Peiyuan Zhang, Kexian Tang, Hao Li, Zicheng Zhang, Guangtao Zhai, Junchi
 677 Yan, Hua Yang, Xue Yang, and Haodong Duan. Envisioning beyond the pixels: Benchmarking
 678 reasoning-informed visual editing. *arXiv preprint arXiv:2504.02826*, 2025.

679

680

681

682

683

684

685

686

687

688

689

690

691

692

693

694

695

696

697

698

699

700

701

702 A MORE DETAILS OF PICABENCH
703704 A.1 TASK DEFINITION
705706 A.1.1 OPTICS
707

708 **Light propagation** requires shadows that are geometrically consistent with the dominant light source,
709 including direction, length, softness, and occlusion. Typical failure modes include misaligned or
710 missing cast shadows and flat shading that ignores occluders.

711 **Reflection** consistency demands view-dependent behavior for specular highlights and mirror reflections.
712 Mirror images must preserve pose and depth; highlight positions should vary with surface
713 curvature and viewpoint. Failures include “floating” reflections or highlights that remain fixed despite
714 evident shape or view changes.

715 **Refraction** requires continuous, coherent background distortion through transparent or translucent
716 media. When edited objects involve glass or water, background edges should bend and scale according
717 to interface geometry, with preserved edge continuity. Discontinuous refractive boundaries or inverted
718 distortions indicate violations.

719 **Light-source effects** evaluate whether new light-introducing edits (like “add a lamp”) are consistent
720 with the global illumination context—color casts, shadow penumbra, and brightness falloff should
721 integrate naturally with the scene. Common issues include mismatched color temperatures, overly
722 hard shadows, or inconsistent falloff relative to distance.

724 A.1.2 MECHANICS
725

726 **Deformation** assesses whether shape changes respect expected material properties. Rigid objects
727 should not bend plastically; elastic deformations should be smooth and bounded. Texture and
728 patterning should warp consistently with geometry rather than tear or duplicate. For instance,
729 changing a chair’s height should not collapse its frame or produce rubber-like bending.

730 **Causality** requires physically plausible contacts and supports under gravity. Edited objects should not
731 float, interpenetrate, or rest in unstable equilibria (e.g., a heavy object balanced on a non-supporting
732 point). Support relations must imply load transfer and stability. Violations include hovering objects,
733 impossible stacking, and intersecting geometries that break solidity.

734 A.1.3 STATE TRANSITION
735

736 **Global transitions** affect the entire scene (e.g., day-to-night, dry-to-wet, solid-to-molten). Changes
737 must propagate consistently: illumination color and intensity should update across surfaces; wetness
738 should alter reflectance and darkening on all relevant materials; phase changes should be coherent
739 and, when implied, justified by scene-level cues (e.g., a pervasive heat source). Inconsistencies
740 include night skies with daylight shadows or partial melting without corresponding global evidence.

741 **Local transitions** involve spatially confined edits (e.g., adding steam, charring an edge, or melting a
742 corner). These effects must integrate with nearby context and causal cues. Steam implies heat and
743 moisture and may induce local condensation; flames produce light spill and secondary reflections;
744 partial melting should respect material boundaries and continuity. When localized changes ignore
745 surrounding context or violate material behavior, the edit becomes physically implausible.

747 A.2 MORE SCORE RESULTS
748

749 Tab. 4 lists the performance of models on PICABench, evaluated by Qwen2.5-VL-72B (Bai et al.,
750 2025). It can be seen that the general rule and conclusion are similar to those suggested by Tab. 1:
751 Most models have very low scores (below 60), indicating a fatal gap in the ability to generate
752 physics-aware images.

753
754 A.3 DETAILS OF BENCHMARK METRICS
755

756 Table 4: **Quantitative comparison on PICABench** evaluated by Qwen2.5VL-72B for instruction-
 757 based editing models, where Acc, Con, LP, LSE, GST, LST denote Accuracy (%) and Consistency
 758 (**db**), Light propagation, Light Source Effects, Global State Transition, Local State Transition respec-
 759 tively. ■ and □

Model	LP		LSE		Reflection		Refraction		Deformation		Causality		GST		LST		Overall	
	Acc	Con	Acc	Con	Acc	Con	Acc	Con	Acc	Con	Acc	Con	Acc	Con	Acc	Con	Acc	Con
GPT-Image-1	54.59	18.81	51.07	20.13	44.85	19.07	45.26	18.64	52.48	20.37	41.14	20.08	56.75	36.20	47.66	22.71	49.94	22.95
Nano Banana	45.05	29.72	38.72	31.39	44.07	26.90	36.86	27.74	48.68	27.42	41.77	28.44	48.53	40.63	44.40	32.81	44.50	31.22
Seedream 4.0	52.30	25.49	53.92	28.27	50.64	23.82	41.46	27.00	45.70	27.27	42.41	26.71	53.62	36.76	47.79	33.20	49.22	29.05
Bagel	36.22	28.57	33.02	32.08	36.98	28.78	34.42	24.31	35.26	28.08	37.34	31.20	36.50	35.15	31.64	32.05	35.28	30.48
Bagel-Think	42.40	31.33	37.53	29.80	36.60	33.01	37.40	27.66	37.58	29.79	36.71	34.11	40.22	36.91	35.68	34.19	38.12	32.70
DiMOO	31.27	27.70	19.24	33.26	22.42	24.00	26.29	23.93	29.47	30.65	30.17	27.39	15.66	49.42	26.04	36.09	24.20	32.73
OmniGen2	42.58	20.46	35.63	28.85	41.11	25.10	33.60	23.22	35.93	25.51	34.39	28.05	36.20	38.52	28.65	27.80	36.08	27.84
Uniworld-V1	33.04	18.89	24.47	20.48	30.67	19.16	21.14	19.06	31.95	19.16	28.06	18.10	18.40	17.54	27.86	19.56	26.68	18.90
Hidream-E1.1	37.81	20.46	32.54	25.38	38.40	20.18	30.62	21.17	35.10	22.37	32.49	22.15	43.44	34.75	34.51	24.17	36.74	24.39
StepIX-Edit	38.52	29.46	34.44	31.26	39.18	29.50	27.64	31.58	39.57	31.51	39.24	32.09	43.74	35.43	32.94	30.19	37.88	31.47
Qwen-Edit	47.88	22.03	44.66	26.28	43.94	23.80	40.11	26.54	41.72	26.42	38.82	24.94	47.16	36.72	41.54	28.44	43.70	27.42
Flux.1 Kontext	41.34	29.21	39.43	29.61	44.72	27.83	28.46	28.22	39.07	31.50	50.63	31.44	40.51	39.03	36.46	33.95	40.44	31.90
Flux.1 Kontext+SFT	45.76	30.42	42.28	30.69	46.13	28.37	32.25	28.40	41.89	31.74	47.05	31.87	40.90	40.82	37.76	34.41	41.96	32.71

We provide detailed definition of accuracy and consistency as follows. Let N be the total number of annotated QA pairs, \hat{a}_i be the VLM-predicted answer for the i -th question, a_i be the reference answer, and $\mathbb{I}(\cdot)$ the indicator function. The accuracy is defined as:

$$\text{Acc} = \frac{1}{N} \sum_{i=1}^N \mathbb{I}(\hat{a}_i = a_i) \quad (1)$$

We use psnr of non-edited region as consistency. For each image pair, we compute the PSNR over non-edited pixels, using a binary mask $M_i(p)$ where $M_i(p) = 1$ denotes an edited pixel and $M_i(p) = 0$ otherwise. Define the non-edited region as $\Omega_i = \{p \mid M_i(p) = 0\}$, where p indexes pixels. Let I_i^{src} be the source image and I_i^{edit} the edited image.

The MSE (mean squared error) over the non-edited region is:

$$\text{MSE}_i = \frac{1}{|\Omega_i|} \sum_{p \in \Omega_i} \|I_i^{\text{edit}}(p) - I_i^{\text{src}}(p)\|_2^2 \quad (2)$$

Then, the per-sample consistency score (PSNR) is:

$$\text{Con}_i = 10 \cdot \log_{10} \left(\frac{\text{MAX}^2}{\text{MSE}_i} \right) \quad (3)$$

Finally, the dataset-level consistency is computed as the average across all N samples:

$$\text{Con} = \frac{1}{N} \sum_{i=1}^N \text{Con}_i \quad (4)$$

Here, MAX is the maximum pixel value (e.g., 255 for 8-bit images).

A.4 DETAILED HUMAN EVALUATION PROTOCOL

Study setup. We use the Rapidata¹ platform to conduct pairwise human preference comparisons for evaluating image editing quality. Each trial presents a reference image and two model outputs (A/B) under a fixed unified instruction:

Select the image that more closely matches the editing instruction.

The A/B order is randomized per trial. Annotators are compensated at or above local minimum wage.

Datasets and models. We evaluate 10 models over the PICABench dataset at three difficulty levels (*superficial*, *intermediate*, *explicit*), forming 45 unordered model pairs per item. For each difficulty,

¹<https://www.rapidata.ai/>

810 we sample 50 items via stratified sampling over the `physics_law` taxonomy. Each item yields 45
 811 comparisons, each judged by 3 annotators, resulting in 20,250 votes per split.
 812

813 **Elo computation.** To aggregate preferences, we use a robust Elo rating system. For a match between
 814 model A and B with current ratings (R_A, R_B) , the expected win probability of A is:
 815

$$E_A = \frac{1}{1 + 10^{\frac{R_B - R_A}{S}}}, \quad (5)$$

817 where $S = 400$ is the scaling factor.
 818

819 Given the vote ratio $s_A \in [0, 1]$ for model A , with $s_B = 1 - s_A$, the ratings are updated as:
 820

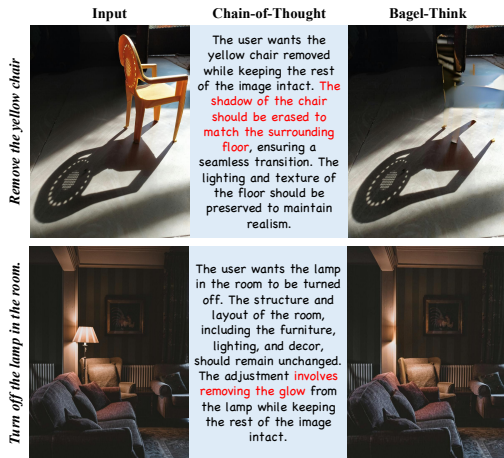
$$\begin{aligned} R'_A &= \max(R_{\min}, R_A + K_{\text{eff}}(s_A - E_A)), \\ R'_B &= \max(R_{\min}, R_B + K_{\text{eff}}(s_B - E_B)), \end{aligned} \quad (6)$$

822 where $K_{\text{eff}} = K \cdot \frac{v}{5}$ adjusts for vote count $v = v_A + v_B$, and $K = 24$ is the base step size.
 823

824 **Robust aggregation.** To reduce order effects and improve stability, we shuffle the comparison stream
 825 and re-run Elo updates for $T = 50$ rounds. The final Elo score for model m is computed as:
 826

$$\bar{R}_m = \frac{1}{T} \sum_{t=1}^T R_m^{(t)}, \quad \sigma_m = \sqrt{\frac{1}{T} \sum_{t=1}^T (R_m^{(t)} - \bar{R}_m)^2}. \quad (7)$$

829 **Parameter setting.** Table 5 summarizes the Elo configuration used in all human evaluations.
 830



846 Figure 7: Examples of Bagel’s reasoning trace.
 847

Table 5: Elo parameter setting.

Parameter	Value
Initial Elo rating	1,000
Elo scaling factor S	400
Base K-factor	24
Minimum Elo rating R_{\min}	700
Number of rounds T	50
Votes per match	3
Model pairs per item	45
Items per difficulty	50
Benchmark splits	3
Total comparisons per split	6,750
Total votes per split	20,250

A.5 MORE VISUALIZATION

851 Fig. 8-11 presents generated images of various models prompted by samples in our PICABench.
 852 The prompts cover all eight physics laws and three complexity levels. They demonstrate that the
 853 performance of these models varies considerably in complying with physical laws.

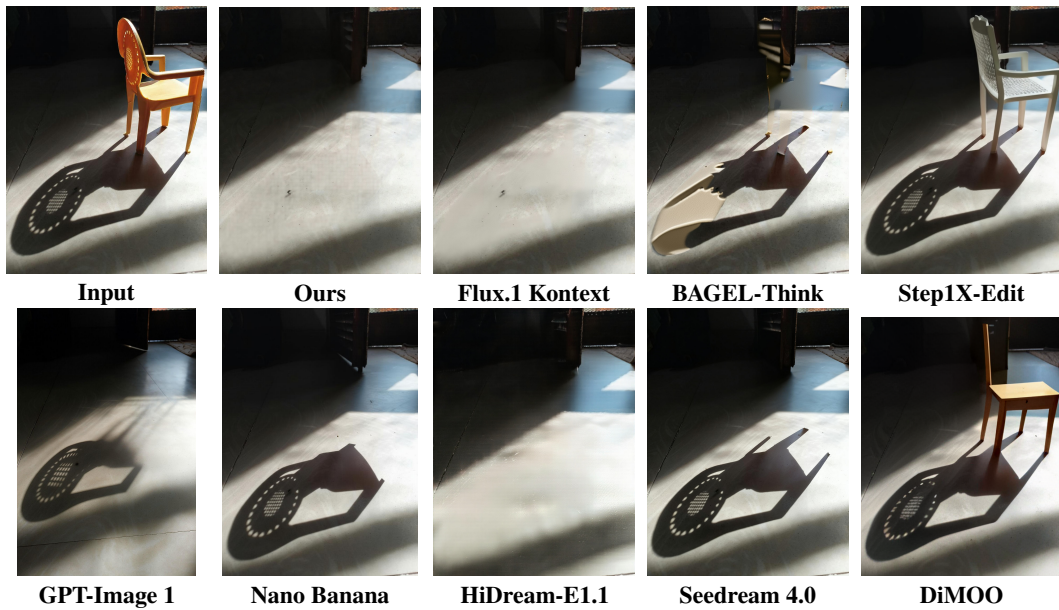
854 Most models either just perform superficial edits and ignore the physics law, or completely fail to
 855 understand the instruction. Only a few models, including ours, can yield physically plausible images
 856 in most cases. Therefore, the ability to follow physical laws is crucial but lacking in most models,
 857 and by PICABench we hope to draw the community’s attention to this critical problem.

858 Moreover, we show Bagel’s think process in Fig. 7. As shown in Fig. 7, model successfully reasons
 859 the correct results in its chain-of-thought, yet fails to execute them in the generated image.
 860

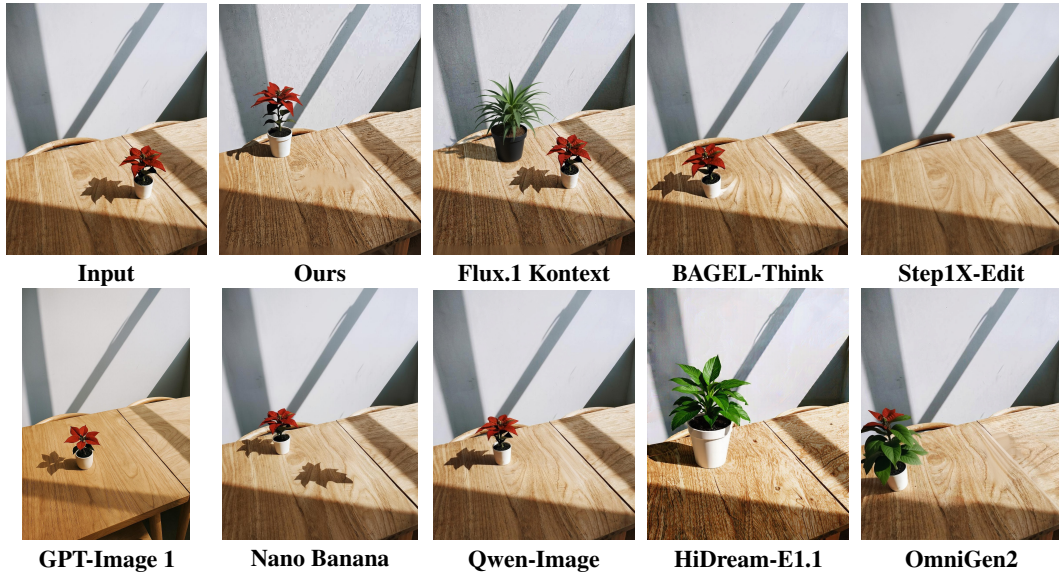
A.6 SYSTEM PROMPT FOR QA GENERATION

861 To generate QA pairs, we design a system prompt as follows.
 862

864 **Superficial Prompt:** Remove the yellow chair



865 **Superficial Prompt:** Move the potted plant to left side of the table.



906 Figure 8: Examples of how models follow the law of light propagation in optics (superficial prompts).

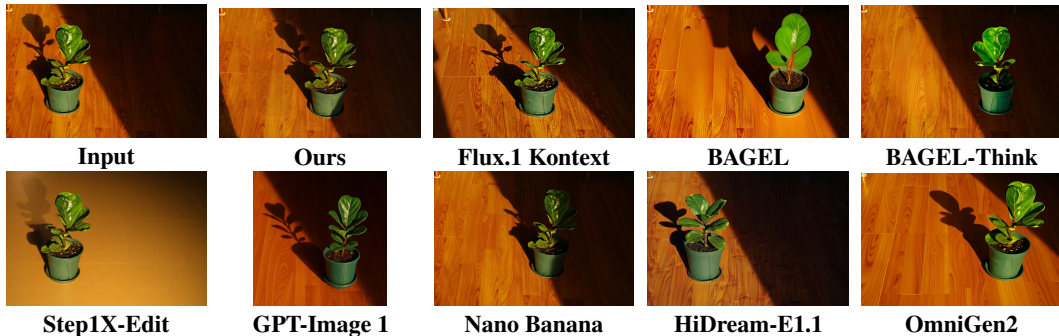
911 System Prompt for QA Generation

912 You are an expert in image editing evaluation. Your task is to generate specific, targeted QA pairs to
 913 assess the success of this image editing task.

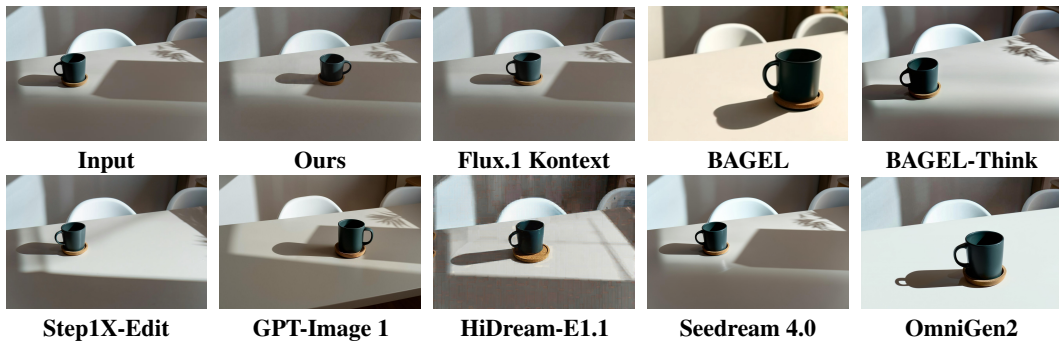
914 **EDITING TASK CONTEXT:**

- 915 - Edit Instruction: {edit_instruction}
- 916 - Physics Law: {physics_law}
- 917 - Operation Type: {operation}

918 **Intermediate Prompt:** Move the potted plant as a whole to the right side of the image, keeping it
 919 upright on the flat ...



920
 921
 922
 923
 924
 925
 926
 927
 928
 929
 930
 931
 932 **Explicit Prompt:** Reposition the dark ceramic mug together with its round cork coaster from its
 933 current spot to the right half of ...



934
 935
 936
 937
 938
 939
 940
 941
 942
 943
 944
 945
 Figure 9: Examples of how models follow the law of light propagation in optics (intermediate &
 946 explicit propmts).

946
 947
CRITICAL CONSTRAINT:

948
 949
 950 The evaluator will ONLY see the final edited image and the edit instruction. They **CANNOT** see the
 951 original image. Therefore, all questions must be answerable based solely on the final image.

952
 953 **GENERATE QUESTIONS FOR TWO CATEGORIES:**

954
 955 **1. EDITING COMPLETION ASSESSMENT**

956 Your goal: verify that the specific changes requested in the instruction are visible in the final image.

957 - Always **explicitly localize** the target object using a locator phrase *within* the noun phrase.
 958 - Locator phrases may use: *position* (left/right/top...), *relative position*, *ordinal* (leftmost...), *attributes*
 959 (color/size...), *relationships* (attached to...).
 960 - Focus on directly observable characteristics in the result.

961
 962 **2. PHYSICS CONSISTENCY ASSESSMENT**

963 Your goal: evaluate whether the final image respects the laws of {physics_law}.

964 - Check for physically impossible or unrealistic arrangements.
 965 - Assess object states, positions, contacts, shadows, reflections, etc.
 966 - Evaluate *current* physical state only, not the editing process.

967
 968 **MANDATORY SINGLE-CRITERION RULE**

969 - Each question must test **exactly one** observable predicate.
 970 - **Do not** use "and", "or", "while", "both", etc.
 971 - Connectors may be used inside locator phrases only.
 972 - Valid predicates: present/absent, is color X, located at Y, touching, casting shadow, number equals N.

973
 974 **QUESTION FORM GUIDELINES**

975 - **Removal:** Ask for absence, e.g., "Is the [locator] [object] absent?"

976 - **Addition:** Ask for presence.

977 - **Move:** Ask for new position relative to anchor.

978 - **Attribute:** Ask for color/texture/text on the object.

972 **Superficial Prompt:** Turn on the lamp on the bedside table.
 973
 974
 975
 976
 977
 978
 979
 980
 981
 982



995
 996 **Superficial Prompt:** Turn off the lamp in the room.
 997
 998
 999
 1000
 1001
 1002
 1003
 1004
 1005



1017 Figure 10: Examples of how models follow the law of light source effects in optics (superficial
 1018 prompts).

1019
 1020
 1021 - **Count:** Ask about exact number of localized targets.
 1022 - Use clear and concrete language. Avoid vague terms like “some”, “appears to”, “looks like”.
 1023

REQUIREMENTS

1024 - Keep questions concise and clear.
 1025 - Use simple language; split complex checks.

1026
 1027 - Avoid ambiguity and ensure single interpretation.
 1028 - Use locator phrases when categories appear multiple times.
 1029 - Frame questions positively.
 1030 - Cover all key aspects with multiple atomic questions (each addressing a different predicate).
CRITICAL: Every answer must be "Yes" or "No" — no other values are acceptable.
OUTPUT FORMAT:

```
1031
1032 {
1033     "Editing Completion QA": [
1034         {"question": "...", "answer": "Yes"},  

1035         {"question": "...", "answer": "No"}  

1036     ],  

1037     "Physics Consistency QA": [  

1038         {"question": "...", "answer": "Yes"},  

1039         {"question": "...", "answer": "No"}  

1040     ]  

1041 }
```

BAD EXAMPLES (DO NOT OUTPUT)

- "Is there a table?" (ambiguous)
- "Is the central table removed and is the floor clean?" (two predicates)

GOOD EXAMPLES

- "Is there a round wooden table in the center foreground?"
- "Is there a small blue cup on the right edge of the desk?"
- "Is there a traffic cone placed on the left side of the crosswalk?"
- "Is the leftmost of the two vases red?"
- "Is the shadow of the lamp cast toward the lower-right, consistent with a top-left light source?"

Final Reminder:
 Questions must evaluate the *final image state*, not the editing history.
 Avoid rewording the same question multiple times — each question must test a **different** aspect.

B MORE DETAILS ABOUT PICA-100K

B.1 SYSTEM PROMPT FOR IMAGE-TO-VIDEO CAPTIONING

To generate physics-aware captions for image-to-video generation, we design a system prompt that instructs the model to describe one physically plausible, visually salient content change observable over 3–5 seconds. The model is not allowed to reference the source image, prompt, or editing. The full system prompt used is shown below.

System Prompt for I2V Caption Generation

You are an expert writer of image-to-video captions (3–5 s).

You will receive ONE input image. DO NOT ask questions. DO NOT mention "image/photo/edit/prompt".

Goal

- Produce ONE concise motion caption that creates a VISUALLY OBVIOUS content change consistent with the physical law.
- "Content change" means change the state of light source (add/remove/move/change color or intensity), add/remove/move/replace an object, or alter a local/global material state.
- The camera is secondary: keep camera static unless a tiny move is necessary for visibility.

Thinking Steps (internal only)

- 1) Parse the scene: pick 1–2 salient objects; identify light, surfaces, supports, deformables, reflective/refractive media.
- 2) Choose ONE change that the specified physical law can plausibly cause. Prefer highly visible ones.
- 3) Make it measurable: include motion/visual cues (e.g., "slides right by half its width", "shadow doubles").
- 4) Keep identities and layout stable unless global changes are implied.
- 5) Default: camera static. If necessary, use one simple motion (e.g., slow push-in).

Law Playbook (pick one)

- Light_Source_Effects: turn on/off lamp; move lamp to affect all lit areas.
- Light_Propagation: move object to change shadow shape/position under key light.

1080
 1081 - Reflection: place object near mirror; reflection should match highlights.
 1082 - Refraction: move object behind glass/water to create distortion.
 1083 - Deformation: add weight to soft object (e.g., pillow) to create indentation.
 1084 - Causality: remove support or add offset weight to cause collapse/tilt/slide.
 1085 - Local: change wet/dry/frozen/burnt/fractured/etc. with local visual cues.
 1086 - Global: simulate time/season/weather shift with coherent lighting/material change.

1086 Constraints

- Duration: 3–5 seconds, single continuous shot.
 - Primary change must be content-based.
 - No object added/removed unless required by the change.
 - Use specific, visible nouns (e.g., “mirror”, “glass of water”, “pillow”).
 - Use physics cue words (e.g., shadow, reflection, warping, indentation).
 - Avoid stories or naming the law.
 - End the sentence with camera state: e.g., “camera static”.

1092 Output Format

1093 Return ONLY valid JSON:

1094 `{"i2v_prompt": "..."}`

1095 Examples (for reference only)

- “The desk lamp turns off and all previously lit areas fall into dimness, camera static.”
 - “The ceramic mug slides right by half its width and its shadow shortens under left key light, camera static.”
 - “The spoon moves behind the glass and warps due to refraction, camera static.”
 - “A dumbbell compresses the pillow, forming a deep indentation and partial rebound, camera static.”
 - “Dense droplets form on the fabric and darken the surface, camera static.”
 - “Light shifts to sunset; shadows grow longer and warmer, camera static.”

1103 **B.2 EXAMPLE OF PICA-100K**

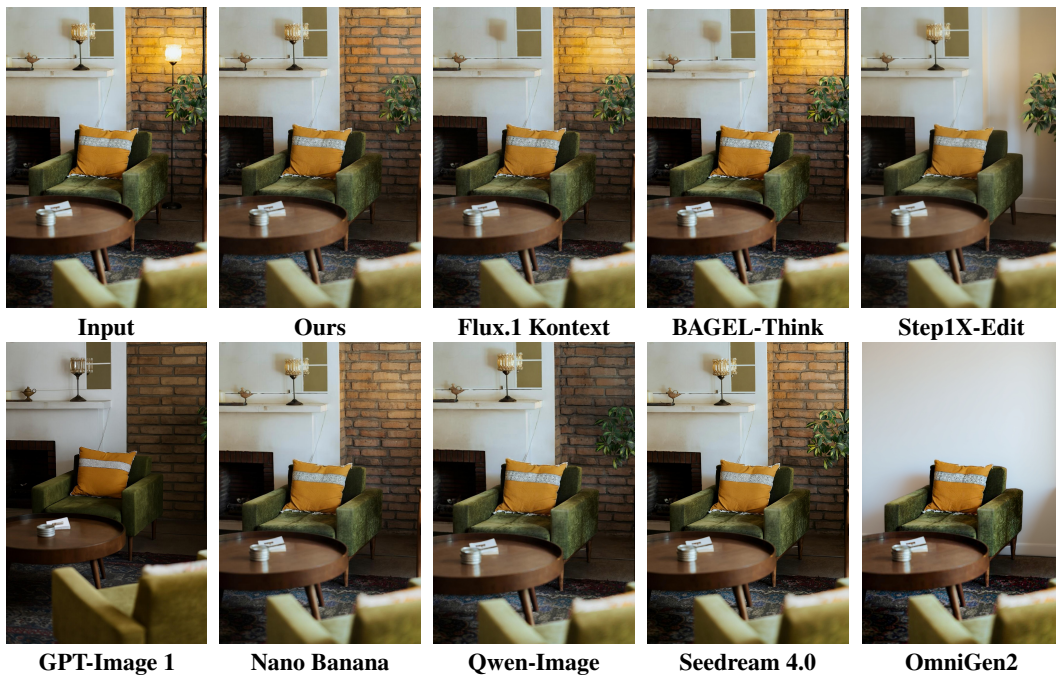
1104 Fig. 12 shows some examples in PICA-100K dataset. For each pair, we focus on the manifestation of
 1105 physical laws.

1106
 1107
 1108
 1109
 1110
 1111
 1112
 1113
 1114
 1115
 1116
 1117
 1118
 1119
 1120
 1121
 1122
 1123
 1124
 1125
 1126
 1127
 1128
 1129
 1130
 1131
 1132
 1133

1134

1135

1136 **Intermediate Prompt:** Remove the tall floor lamp next to the plant on the right and also remove all
 1137 illumination it produced. Update ...



1148

1149

1150

1151

1152

1153

1154

1155

1156

1157

1158

1159

1160

1161

1162

1163 **Explicit Prompt:** In the snowy dusk forest scene, a wooden post at center-left carries two lanterns,
 1164 with the upper-left lantern currently glowing ...



1173

1174

1175

1176

1177

1178

1179

1180

1181

1182

1183

1184

1185

1186

1187

1188 Figure 11: Examples of how models follow the law of light source effects in optics (intermediate &
 1189 explicit prompts).

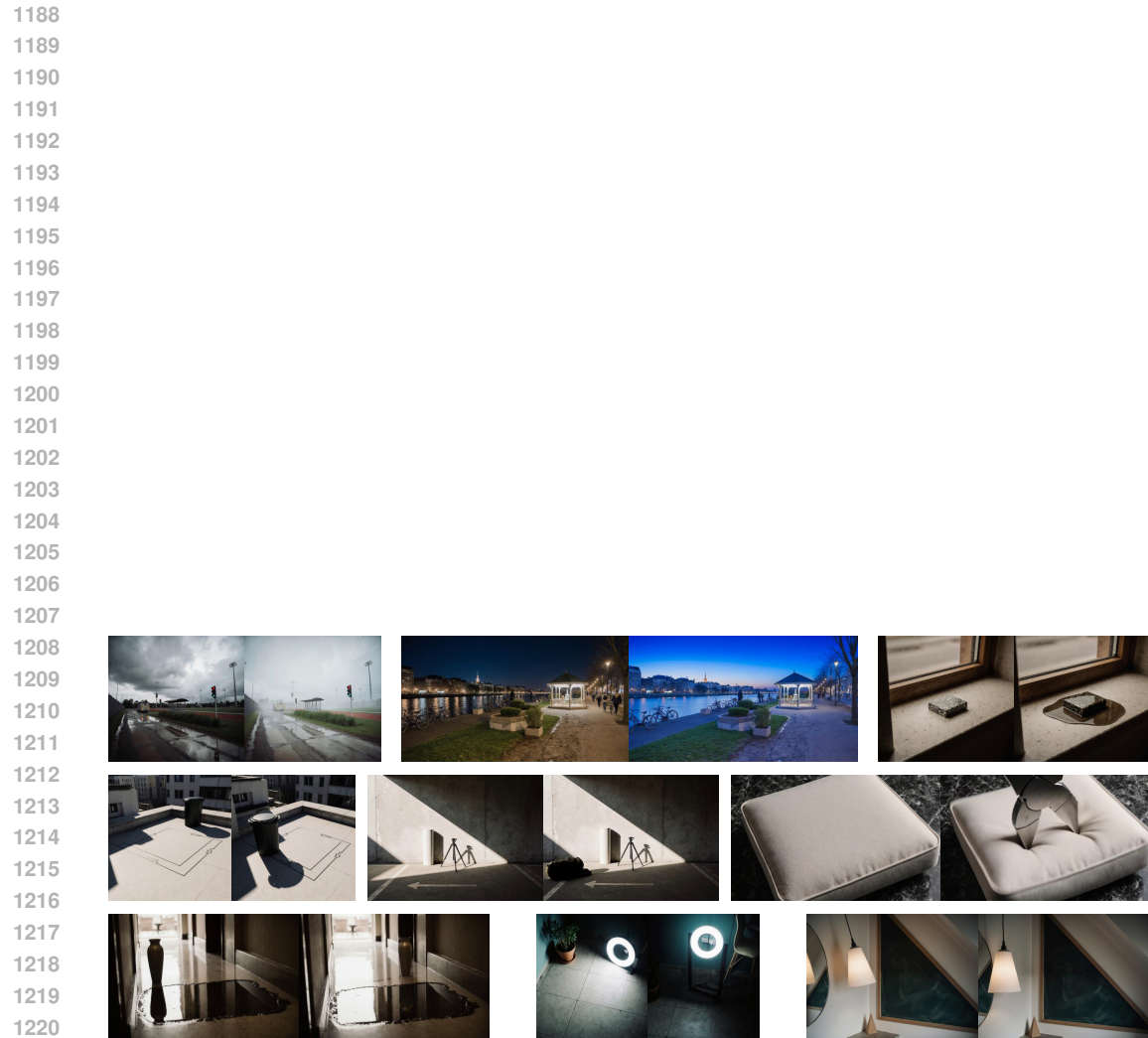


Figure 12: Examples of PICA-100K dataset.